

## New Topology in Azide-Bridged Cobalt(II) Complexes: the Weak Ferromagnet $[\text{Co}_2(\text{N}_3)_4(\text{Hexamethylenetetramine})(\text{H}_2\text{O})]_n$

Franz A. Mautner,<sup>†</sup> Lars Öhrström,<sup>‡</sup> Beate Sodin,<sup>†</sup> and Ramon Vicente<sup>\*§</sup>

<sup>†</sup>*Institut für Physikalische und Theoretische Chemie, Technische Universität Graz, Rechbauerstrasse 12, A-8010, Graz, Austria,* <sup>‡</sup>*Department of Chemical and Biological Engineering, Chalmers Tekniska Högskola, SE-412 96 Göteborg, Sweden,* and <sup>§</sup>*Departament de Química Inorgànica, Universitat de Barcelona, Martí i Franquès 1-11, 08028 Barcelona, Spain*

Received March 19, 2009

A new polynuclear azido-bridged Co(II) compound with formula  $[\text{Co}_2(\text{N}_3)_4(\text{HMTA})(\text{H}_2\text{O})]_n$  (**1**) (HMTA = hexamethylenetetramine) has been structurally and magnetically characterized. The compound **1** crystallizes in the monoclinic system  $C2/m$  space group, and consist of a complex three-dimensional system in which end-to-end and end-on azido bridging ligands between the Co(II) atoms coexist. The HMTA ligand is also linking three different Co(II) atoms. The network analysis shows for **1** a three- and six-connected network topology not previously reported. The magnetic properties of **1** are also reported, and it was found that the magnetic interactions define another new three- and four-connected net assigned as a  $(6.8^2)(6^4 \cdot 10^2)$ -**tfo** net. In the high temperature region the  $\chi_M$  versus  $T$  plot can be fitted by using the Curie–Weiss law, and the best fit theta value is  $-26.6$  K. For **1** magnetic ordering and spontaneous magnetization is achieved below  $T_c = 15.6$  K.

### Introduction

The number of one-dimensional (1D) to three-dimensional (3D) azido bridged Co(II) compounds<sup>1–16</sup> is quickly increasing mainly after the report of the double end-on (EO) azide bridged single-chain magnet (SCM)  $[\text{Co}(2,2'\text{-bithiazoline})$

$(\text{N}_3)_2]$ .<sup>4</sup> Another SCM azido-bridged Co(II) compound has been reported recently,<sup>14</sup> and, on the other hand, the combination of the anisotropic Co(II) cation with the coordination versatility and the consequent different superexchange coupling ways of the azido bridging ligand has produced several compounds having unusual properties in their combinations of magnetism and structure as multi-layer systems with complex long-range magnetic ordering behavior,<sup>16</sup> the compound  $[\text{Co}(\text{bpg})(\text{N}_3)_2] \cdot (\text{DMF})_{4/3}$  (bpg = meso- $\alpha,\beta$ -bi(4-pyridyl)glycol) showing a Kagomé layer<sup>5</sup> or the weak ferromagnet  $[\text{Co}(\mu_{1,3}\text{-N}_3)_2(4\text{-acpy})_2]_n$  (4-acpy = 4-acetylpyridine).<sup>10,11</sup>

In this paper, we report the synthesis and magnetic properties of a new Co(II) azido compound forming a 3D coordination network:  $[\text{Co}_2(\text{N}_3)_4(\text{HMTA})(\text{H}_2\text{O})]_n$  (**1**) (HMTA = hexamethylenetetramine). **1** shows a complex structure in which coexist Co(II) atoms linked by end-to-end azido bridging ligands, by end-on azido bridging ligands, and by the HMTA ligand acting as tridentate bridging ligand. From the point of view of the magnetic properties, **1** is a bulk antiferromagnetically coupled system in which spontaneous magnetization is achieved below  $T_c = 15.6$  K. The canting angle,  $\gamma$ , has been roughly calculated<sup>11</sup> from the powder direct current (dc) magnetic measurements to be  $7.2^\circ$ . Taking into account the complex structure of **1** and the fact that the coupling through EE and EO azido bridging ligands is usually antiferromagnetic (AF) or ferromagnetic (F) respectively (no magnetic coupling is expected through the HMTA bridging ligand), we have performed a network analysis for **1**

\*To whom correspondence should be addressed. E-mail: ramon.vicente@qi.ub.es. Fax: +34 934907725.

- (1) Viau, G.; Lombardi, M. G.; De Munno, G.; Julve, M.; Lloret, F.; Faus, J.; Caneschi, A.; Clemente-Juan, J. M. *Chem. Commun.* **1997**, 1195.
- (2) Hong, C. S.; Koo, J.-e.; Son, S.-K.; Lee, Y. S.; Kim, Y.-S.; Do, Y. *Chem. Eur. J.* **2001**, 7, 4243.
- (3) Doi, Y.; Ishida, T.; Nogami, T. *Bull. Chem. Soc. Jpn.* **2002**, 75, 2455.
- (4) Liu, T.-F.; Fu, D.; Gao, S.; Zhang, Y.-Z.; Sun, H.-L.; Su, G.; Liu, Y.-J. *J. Am. Chem. Soc.* **2003**, 125, 13976.
- (5) Wang, X.-Y.; Wang, L.; Wang, Z.-M.; Gao, S. *J. Am. Chem. Soc.* **2006**, 128, 674.
- (6) Liu, F.-C.; Zeng, Y.-F.; Jiao, J.; Bu, X.-H.; Ribas, J.; Batten, S. R. *Inorg. Chem.* **2006**, 45, 2776.
- (7) Liu, T.; Zhang, Y.; Wang, Z.; Gao, S. *Inorg. Chem.* **2006**, 45, 2782.
- (8) Yoo, H. S.; Kim, J. I.; Yang, N.; Koh, E. K.; Park, J.-G.; Hong, C. S. *Inorg. Chem.* **2007**, 46, 9054.
- (9) Wang, X.-T.; Wang, Z.-M.; Gao, S. *Inorg. Chem.* **2007**, 46, 10452.
- (10) Abu-Youssef, M. A. M.; Mautner, F. A.; Vicente, R. *Inorg. Chem.* **2007**, 46, 4654.
- (11) Wang, X.-Y.; Wang, Z.-M.; Gao, S. *Inorg. Chem.* **2008**, 47, 5720.
- (12) Mondal, K. C.; Sengupta, O.; Nethaji, M.; Mukherjee, P. S. *Dalton Trans.* **2008**, 767.
- (13) Li, R.-Y.; Wang, X.-Y.; Liu, T.; Xu, H.-B.; Zhao, F.; Wang, Z.-M.; Gao, S. *Inorg. Chem.* **2008**, 47, 8134.
- (14) Sun, H.-L.; Wang, Z.-M.; Gao, S. *Chem. Eur. J.* **2009**, 15, 1757.
- (15) Wang, X.-T.; Wang, X.-H.; Wang, Z.-M.; Gao, S. *Inorg. Chem.* **48**, 2009, 1301.
- (16) Gao, E.-Q.; Liu, P.-P.; Wang, Y.-Q.; Yue, Q.; Wang, Q.-L. *Chem. Eur. J.* **2009**, 15, 1217.

as bulk compound to best understand the structure and also an analysis of the magnetic network for **1**, to try to justify the magnetic properties. The 3D-nets formed in **1** are of some importance, as they show topologies not previously reported. Especially the magnetic net, as this is a highly symmetric network built from nodes with geometries easily obtainable from various "secondary building units" and molecular building blocks. The present case seems to be the first assigned example of this net in chemistry.

## Experimental Section

**Starting Materials.** Co(II) chloride hexahydrate, HMTA, and sodium azide (Aldrich) were used as obtained. Aqueous hydrazoic acid is obtained with a modified Kipp's generator by decomposition of  $\text{NaN}_3$  in  $\text{H}_2\text{SO}_4/\text{H}_2\text{O}$  (1:3, v:v) and subsequent transfer of  $\text{HN}_3$  into  $\text{H}_2\text{O}$  with aid of an inert-gas stream.<sup>17,18</sup>

**Caution!** Hydrazoic acid and Azide compounds are potentially explosive. Only a small amount of material should be prepared, and it should be handled with care.

**Spectral and Magnetic Measurements.** Infrared spectra ( $4000\text{--}400\text{ cm}^{-1}$ ) were recorded from KBr pellets on a Perkin-Elmer 380-B spectrophotometer. Magnetic susceptibility measurements under several magnetic fields in the temperature range  $2\text{--}300\text{ K}$  and magnetization measurements in the field range of  $0\text{--}5\text{ T}$  were performed with a Quantum Design MPMS-XL SQUID magnetometer at the Magnetochemistry Service of the University of Barcelona. All measurements were performed on powdered polycrystalline samples. Pascal's constants were used to estimate the diamagnetic corrections, which were subtracted from the experimental susceptibilities to give the corrected molar magnetic susceptibilities.

**Synthesis.**  $[\text{Co}_2(\text{N}_3)_4(\text{HMTA})(\text{H}_2\text{O})]_n$  (**1**). Sodium azide (0.293 g, 4.5 mmol)  $\text{CoCl}_2 \cdot 6\text{H}_2\text{O}$  (0.480 g, 2.02 mmol) and HMTA (0.280 g, 2.00 mmol) were dissolved in minimum amount of aqueous hydrazoic acid (21 mL) to obtain a clear red solution upon heating to  $70\text{ }^\circ\text{C}$ . Transparent red crystals of **1** were separated by slow cooling of the solution to  $4\text{ }^\circ\text{C}$  within 2 days. (yield approximately 0.375 g, 83.7%) Anal. Found: C, 16.0; H, 3.0; Co, 26.4; N, 50.7. Calcd for  $\text{C}_6\text{H}_{14}\text{Co}_2\text{N}_{16}\text{O}$  (444.19): C, 16.2; H, 3.2; Co, 26.5; N, 50.5. IR (KBr,  $\text{cm}^{-1}$ ): 3408 vw, 3351 vw, 3007 vw, 2961 vw, 2084 vs ( $\nu_{\text{as}}\text{N}_3$ ), 1451 w, 1359 w, 1297 w, 1233 m, 1228 w, 1061 w, 1005 m, 973 m, 915 w, 844 w, 797 m, 774 w, 692 m, 662 w, 614 w, 511 w, 425 w ( $\nu$  = very,  $s$  = strong,  $m$  = medium,  $w$  = weak).

From the synthetic point of view, it should be emphasized that a compound of formula  $[\text{Co}(\text{N}_3)_2(\text{HMTA})(\text{H}_2\text{O})_2]_n$  has been obtained under controlled hydrothermal synthesis.<sup>19</sup> This compound is a 1D infinite polymeric chain in which the HMTA acts as bidentate bridging ligand, and the azido is only a terminal ligand.

**Structure Determination.** A suitable single crystal of **1** (approximately size:  $0.26 \times 0.18 \times 0.12\text{ mm}$ ) was selected for X-ray diffraction. Intensity data were collected with a Bruker AXS KAPPA APEX II diffractometer using graphite monochromated  $\text{Mo-K}\alpha$  radiation. Data were collected at  $100\text{ K}$  using  $\omega$ -scans. Cell parameters were retrieved and refined using Bruker SMART and SAINT software programs. Absorption correction was applied using SADABS. The structure was solved by direct methods by using the SHELXS-86 program and was refined with SHELXL-93 incorporated in the SHELXTL/PC software package. Relevant structural data are given in Table 1. Hydrogen

**Table 1.** Relevant Crystal Data for **1**

empirical formula	$\text{C}_6\text{H}_{14}\text{Co}_2\text{N}_{16}\text{O}$
formula weight	444.19
cryst system	monoclinic
space group	$C2/m$
$a$ (Å)	11.708(2)
$b$ (Å)	12.641(3)
$c$ (Å)	9.482(2)
$\alpha$ (deg)	90
$\beta$ (deg)	90.03(3)
$\gamma$ (deg)	90
$V$ (Å <sup>3</sup> )	1403.3(5)
$Z$	4
$\rho_{\text{calcd}}$ ( $\text{g}\cdot\text{cm}^{-3}$ )	2.102
$F(000)$	896
no. reflections coll.	5579
no. reflections unique	1486
$R_1, wR_2$ (obs. refls)	0.0448, 0.0944
$R_1, wR_2$ (all data)	0.0520, 0.0973
GOF	1.114

**Table 2.** Selected Bond Lengths (Å) and Bond Angles (deg) for **1**<sup>a</sup>

Co1–N11A	2.093(3)	Co1–N21C	2.123(3)
Co1–O1	2.159(4)	Co1–N1	2.201(4)
Co2–N23D	2.059(3)	Co2–N31D	2.148(3)
Co2–N2G	2.370(3)	Co2–N2F	2.370(3)
N11–N12	1.206(6)	N12–N13	1.130(7)
N21–N22	1.172(4)	N22–N23	1.187(4)
N32–N31E	1.188(3)	N2–Co2B	2.370(3)
N11A–Co1–N11	77.0(2)	N11A–Co1–N21	167.47(12)
N11–Co1–N21	91.97(13)	N21–Co1–N21C	98.3(2)
N11A–Co1–O1	87.82(9)	N21–Co1–O1	85.80(11)
N11–Co1–N1	100.83(9)	N21–Co1–N1	86.94(11)
O1–Co1–N1	168.9(2)	N23D–Co2–N31D	90.46(12)
N23–Co2–N2G	91.59(11)	N31–Co2–N2G	92.08(11)
N12–N11–Co1	128.50(9)	Co1A–N11–Co1	103.0(2)
N13–N12–N11	180.0	N22–N21–Co1	134.1(3)
N21–N22–N23	177.9(4)	N22–N23–Co2	123.4(3)
N32–N31–Co2	129.2(2)	N31–N32–N31E	178.1(5)

<sup>a</sup>Symmetry codes: (A)  $-x + 1, -y + 1, -z$ ; (B)  $x, y, z - 1$ ; (C)  $x, -y + 1, z$ ; (D)  $-x + 3/2, -y + 3/2, -z + 1$ ; (E)  $-x + 1, y, -z + 1$ ; (F)  $x, y, z + 1$ ; (G)  $-x + 3/2, -y + 3/2, -z$ .

atoms of the HMTA ligand were inserted in calculated positions. Full-matrix least-squares refinement on  $F^2$  with anisotropic thermal motion parameters for all the non-hydrogen atoms and isotropic for the remaining atoms were employed.<sup>20</sup> Selected bond parameters are summarized in Table 2.

**Network Analysis.** Abbreviations (three-letter codes) for 3D nets were taken from the web-based Reticular Chemistry Structure Resource, where crystallographic coordinates and other useful details for 3D-nets can be obtained.<sup>21</sup> More unusual and exotic nets with confirmed occurrence in known structures are listed in the TTO collection obtainable with the TOPOS program, also used to established the topologies of the nets in **1**.<sup>22,23</sup> The six- and three-connected net in **1** has been given the **loh1** symbol in the TTO collection. Mathematically derived nets can

(20) (a) Blessing, R. H. *Acta Crystallogr.* 1995, A51, 33. SADABS; Bruker AXS: Madison, WI, 1998. (b) Sheldrick, G. M. SHELXS-86, Program for the Solution of Crystal Structure; University of Goettingen: Goettingen, Germany, 1986. (c) Sheldrick, G. M. SHELXL-93, Program for the Refinement of Crystal Structure; University of Goettingen: Goettingen, Germany, 1993. (d) SHELXTL 5.03 (PC-Version), Program library for the Solution and Molecular Graphics; Siemens Analytical Instruments Division: Madison, WI, 1995.

(21) O'Keefe, M.; Yaghi, O. M.; Ramsden, S. Reticular Chemistry Structure Resource; Australian National University Supercomputer Facility: <http://rcsr.anu.edu.au/>, February 2009

(22) Blatov, V. A.; Shevchenko, A. P.; Serezhkin, V. N. *J. Appl. Crystallogr.* 2000, 33, 1193.

(23) TOPOS website: <http://www.topos.ssu.samara.ru/>, Ac. Pavlov St. 1, 443011 Samara, Russia, February 2009.

(17) Bitschnau, B.; Egger, A.; Escuer, A.; Mautner, F. A.; Sodin, B.; Vicente, R. *Inorg. Chem.* 2006, 45, 868, and references therein.

(18) *Energetic Materials*; Fair, H. D., Walker, R. F., Eds.; Plenum Press: New York, 1977; Vol. I, pp 25–31.

(19) Chakraborty, J.; Samanta, B.; Rosair, G.; Gramlich, V.; Salah El Fallah, M.; Ribas, J.; Mitra, S. *Polyhedron* 2006, 25, 3006.

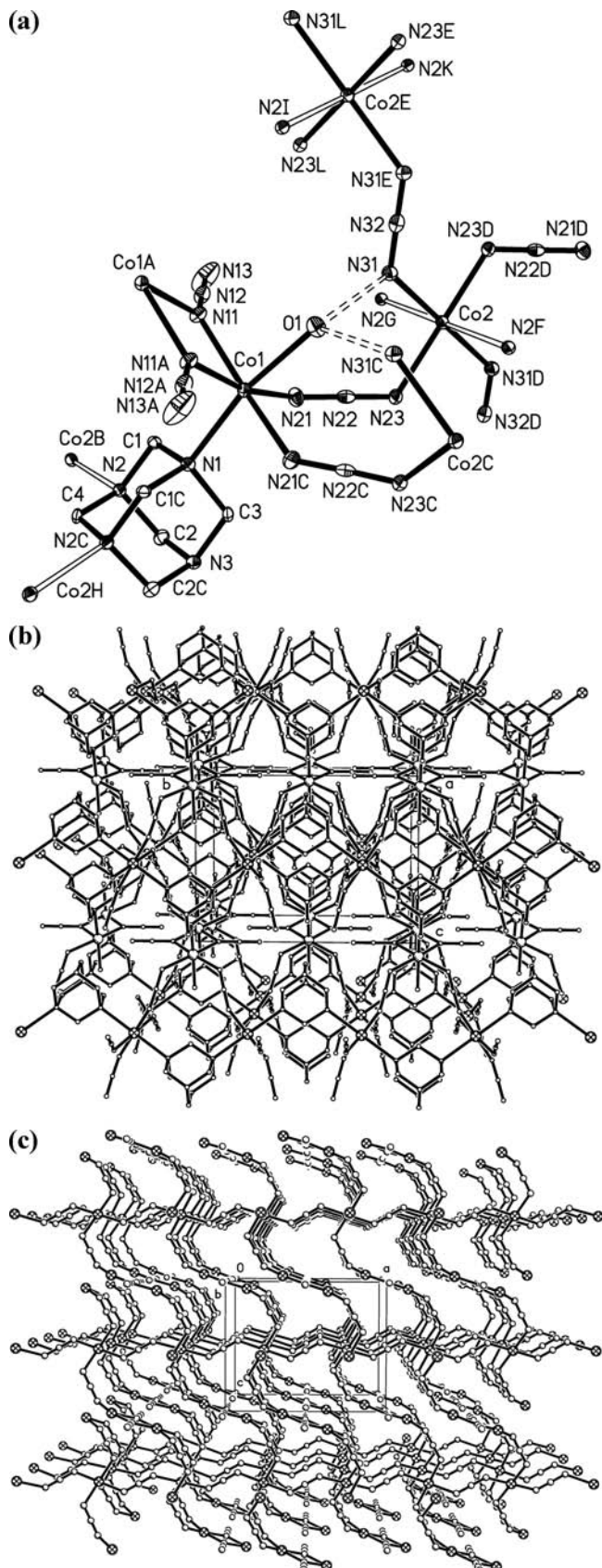


**Figure 1.** (a) ORTEP view of **1** (50% thermal ellipsoids) with atom numbering scheme. (A)  $-x + 1, -y + 1, -z$ ; (B)  $x, y, z - 1$ ; (C)  $x, -y + 1, z$ ; (D)  $-x + 3/2, -y + 3/2, -z + 1$ ; (E)  $-x + 1, y, -z + 1$ ; (F)  $x, y, z + 1$ ; (G)  $-x + 3/2, -y + 3/2, -z$ ; (H)  $-x + 3/2, y - 1/2, -z$ ; (I)  $-x + 1, y, -z$ ; (K)  $x - 1/2, -y + 3/2, z + 1$ ; (L)  $x - 1/2, -y + 3/2, z$ . Hydrogen bonds are indicated by broken bonds. (b) Packing plot of **1** viewed along the  $a$ -axis of the unit cell. (c) The Co(ii)-azide-sublattice of **1** viewed along the  $b$ -axis of the unit cell.

be searched in the EPINET database.<sup>24</sup> For the less common nets the short (Schläfli)<sup>25</sup> symbol before the three-letter code was included for clarity as in  $6^4.8^2$ -nbo. This notation reveals the number of smallest rings found in the net, and, for nets with more than two nodes, also identifies the stoichiometry of the nodes, and the type of network in question. The ideal geometry of the new nets was obtained using SYSTRE.<sup>26</sup>

## Results and Discussion

**Synthesis.** The reaction of Co(II) salt, with HMTA and  $\text{NaN}_3$  in aqueous hydrazoic medium afforded the formation of the title complex **1**, whereas the previously reported  $[\text{Co}(\text{N}_3)_2(\text{HMTA})(\text{H}_2\text{O})_2]_n$ ,<sup>19</sup> has been obtained under controlled hydrothermal conditions. The use of diluted hydrazoic acid allows formation of an acidic medium with pH value  $< 5.5$  without introducing a foreign ion and prevents the quick precipitation of **1** in microcrystalline form.

**Structure of 1.** A perspective view together with the atom numbering scheme of complex **1** is shown in Figure 1a, a packing plot in Figure 1b, and the packing plot of Co-azido-sublattice in Figure 1c. Selected bond distances and bond angles are listed in Table 2. In the structure there exist two cobalt(II) centers: Co1 with ( $z$ -coordinate  $\pm 0.056$ ) and Co2 ( $z$ -coordinate =  $1/2$ ) on inversion center of space group  $C2/m$  and  $Z = 4$ . Co1 is six-coordinated by N1 of the HMTA and by O1 of the aqua ligand, further by N11 and N11A of two EO azide bridges, and in addition by N21 and N21C of the two EE-azide bridges. Co2 is six-coordinated by N23, N31, N23D, N31D of 4 EE-azide bridges and trans coordinated HMTA nitrogen atoms N2G, N2F. The HMTA molecule acts as tridentate bridge between Co1, Co2B, and Co2H. The aqua ligand forms hydrogen bonds of type  $\text{O}-\text{H}\cdots\text{N}$  to N31 and N31C, respectively.

The 3D network of the structure is defined by the HMTA nodes connecting two Co2 atoms and one Co1–Co1 dimer, the Co2 atoms connecting two HMTA and four Co1–Co1 dimers, and the Co1–Co1 dimers connecting two HMTA ligands and four Co2 atoms. This gives a three- and six-connected 3D net, and the nodes and link definitions are shown in Scheme 1.

The resulting network is shown in Figure 2 left. This 3D net was found to have vertex symbols  $4\cdot 4\cdot 4$  for the trigonal nodes and  $4\cdot 4\cdot 4\cdot 4\cdot 4\cdot 4\cdot 6_2\cdot 6_2\cdot 6_2\cdot 6_2\cdot 6_4\cdot 6_4\cdot 8_8\cdot 8_{28}\cdot 8_{28}$  for the octahedral nodes. Although the structure contains two chemically different six-connected nodes, these two are equivalent from the topology point of view. The highest possible symmetry of this net can be calculated, and this indeed results in a 3D-net with space group  $R\bar{3}m$  and only two different nodes, one three-connected and one six-connected, see Figure 2 right.

**Magnetic Network.** As the exchange interaction through the HMTA ligand can be considered as negligible,<sup>19</sup> the magnetic net is reduced in complexity as this node can be deleted. On the other hand, from the magnetic point of view it is necessary to consider the Co1–Co1 dimer as two separate nodes. Thus, we build the net

(24) Hyde, S. T. [epinet.anu.edu.au](http://epinet.anu.edu.au) (accessed Sept. 16, 2008).

(25) O'Keeffe, M.; Eddaoudi, M.; Li, H. L.; Reinecke, T.; Yaghi, O. M. J. *Solid State Chem.* **2000**, *152*, 3–20.

(26) SYSTRE; Delgado Friedrichs, O., 2007; <http://gavrog.sourceforge.net/>.

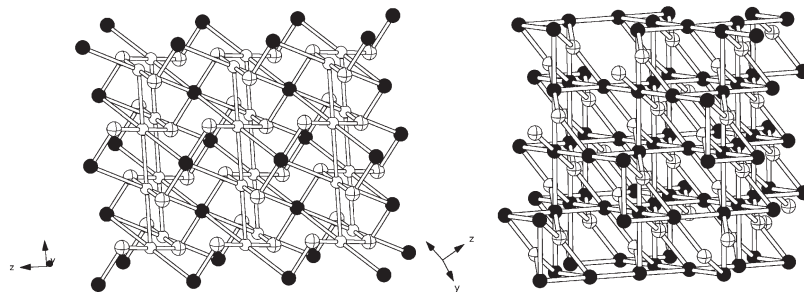
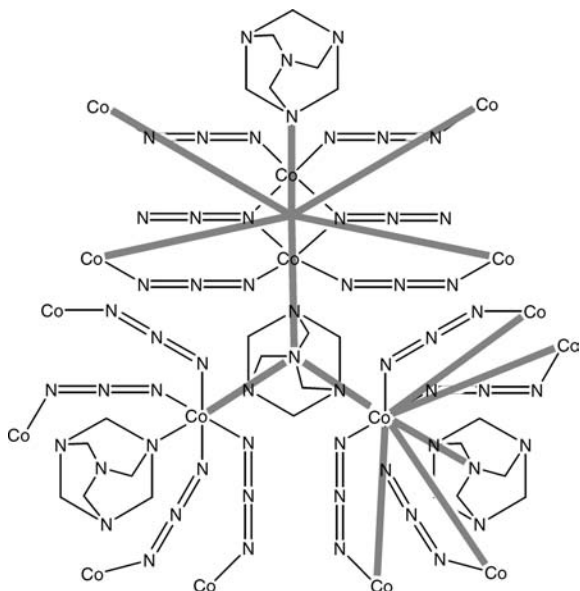


**Figure 2.** (Left) Net in **1**, black spheres, six-connected Co1–Co1 dimers; white spheres, six-connected Co2; crossed spheres, three-connected HMTA ligands. (Right) Ideal net contains only two types of nodes, black spheres, six-connected; crossed spheres, three-connected.

**Scheme 1.** Structural Network in **1**<sup>a</sup>



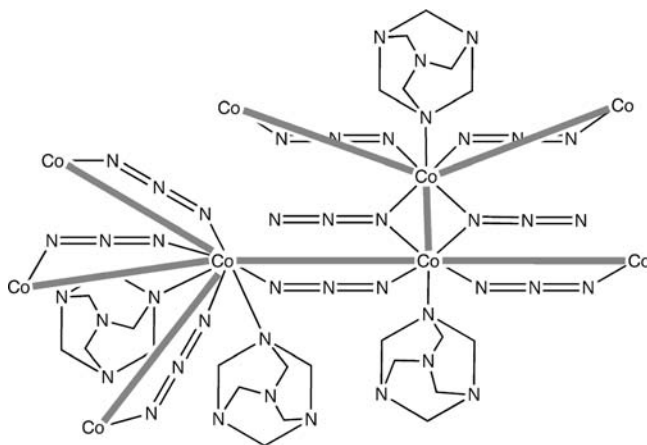
<sup>a</sup>The gray lines define the links between the network nodes: a six-connected at Co2 and at the Co1 dimer, and a three-connected at the HMTA ligand.

from links (couplings) between Co1–Co1 and Co2 via the end-to-end azides and the Co1–Co1 coupling transmitted by the end-on azides. This results in the nodes and links definition shown in Scheme 2 below.

This results in a three- and four-connected net with vertex symbols  $6_2 \cdot 8_2 \cdot 8_2$  for the trigonal nodes and  $6 \cdot 6 \cdot 6 \cdot 6 \cdot 10_2 \cdot 10_2$  for the square planar nodes (Figure 3, left) with topology symbol **tfo**.<sup>21</sup> This 3D-net in its highest possible symmetry has space group  $F_{mmm}$  and almost ideal trigonal planar and square planar nodes (the trigonal angles deviate somewhat:  $126.4^\circ$ ,  $126.4^\circ$  and  $107.2^\circ$ ), see Figure 3 right.

**Discussion of the Networks.** Originally proposed by A. F. Wells in the 1950s,<sup>27</sup> network analysis is emerging as an important tool in understanding crystal structures with strong intermolecular interactions such as coordination polymers.<sup>28–30</sup> In the deliberate synthesis of metal-organic framework compounds, so-called MOFs, the

**Scheme 2.** Magnetic Network in **1**<sup>a</sup>



<sup>a</sup>The gray lines define the links between the network nodes: a four-connected at Co2 and a three-connected at Co1. There is no magnetic coupling transmitted through the HMTA ligand, thus this link is not part of the magnetic net.

theoretical nets serve as blue prints,<sup>31</sup> and the ultimate goal, from a synthetic point of view, is to be able to choose a particular 3D net, find out the geometrical requirements of the nodes and links, and then go into the laboratory and mix the molecular building blocks corresponding to these requirements.

In this latter respect, the use of binodal nets combining high and low connectivity has recently been suggested as a way of obtaining porous materials.<sup>32</sup> One possible class of this type is the three- and six-connected nets. Batten and co-workers have recently reported a number of these and discussed the possibilities with this node combination,<sup>33</sup> and other recent examples have been reported by Cordes and Hanton<sup>34</sup> and by Miller and co-workers.<sup>35</sup> The present compound is not porous and cannot be classified as a MOF; however, the network formed in **1** is of some interest, as it is of a topology not previously reported. The stoichiometry of this net is  $(3\text{-connected})_2(6\text{-connected})_3$  and is thus different from the most common of these nets that have equal numbers

(31) Yaghi, O. M.; Ockwig, N. W.; Chae, H. K.; Eddaoudi, M.; Kim, J. *Nature* **2003**, *423*, 705–714.

(32) Borel, C.; Håkansson, M.; Öhrström, L. *CrystEngComm* **2006**, *8*, 666–669.

(33) Du, M.; Zhang, Z. H.; Tang, L. F.; Wang, X. G.; Zhao, X. J.; Batten, S. R. *Chem. Eur. J.* **2007**, *13*, 2578–2586.

(34) Cordes, D. B.; Hanton, L. R. *Inorg. Chem.* **2007**, *46*, 1634–1644.

(35) Zhu, Q.; Arif, A. M.; Öhrström, L.; Miller, J. S. *J. Mol. Struct.* **2008**, *890*, 41–47.

(27) Wells, A. F. *Acta Crystallogr.* **1954**, *7*, 535–44.

(28) O'Keeffe, M.; Yaghi, O. M. *J. Solid State Chem.* **2005**, *178*, V–VI.

(29) Ockwig, N. W.; Delgado-Friedrichs, O.; O'Keeffe, M.; Yaghi, O. M. *Acc. Chem. Res.* **2005**, *38*, 176–182.

(30) Öhrström, L.; Larsson, K. *Molecule-Based Materials: The Structural Network Approach*; Elsevier: Amsterdam, 2005.

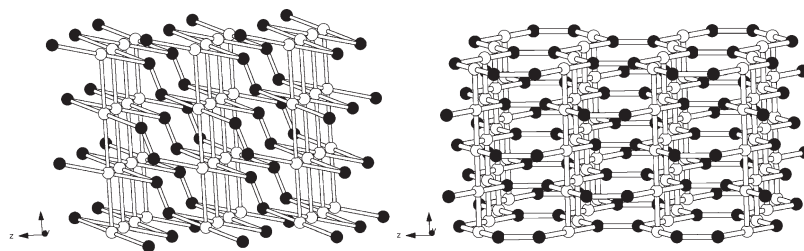


**Figure 3.** (Left) Magnetic net in **1**, black spheres, three-connected Co1; white spheres, four-connected Co2. (Right) Ideal net, black spheres, three-connected; white spheres, six-connected.

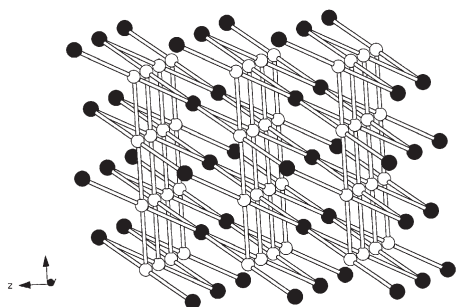


**Figure 4.** Reduced magnetic net in **1**, is of the niobium oxide or  $6^4.8^2\text{-nbo}$  topology. Black spheres are Co1–Co1 dimers and white spheres are Co2 atoms.

of nodes, namely, the  $(4.6^2)(4^2.6^{10}.8^3)\text{-rtl}$  (or rutile) net and the  $(6^3)(6^{12}.8^3)\text{-pyr}$  (or pyrite) net. This stoichiometry means that every six-connected node links to four other six-connected nodes and two three-connected nodes, while the three-connected nodes only link to six-connected nodes. Of the 17 reported six-connected and three-connected nets in the Reticular Chemistry Structure Resource (RCSR) database,<sup>36</sup> none exists with this particular relation between the nodes.

We note that HMTA has been observed as a three-connected node before.<sup>37</sup>

The magnetic net is possibly of more importance, as this is a highly symmetric net built from nodes with geometries easily obtainable from various “secondary building units” (SBUs) and molecular building blocks. The present case seems to be the first assigned example of this net in chemistry, although six earlier examples have been found in the database searches of Blatov and co-workers,<sup>38–40</sup> and it has also been mathematically predicted.<sup>24</sup>

A further reduction in complexity can be achieved if we consider the Co1–Co1 dimer as a one high spin entity. This unites the two three-connected nodes into one four connected node, and the resulting network is of the niobium oxide or  $6^4.8^2\text{-nbo}$  topology, see Figure 4.

**Magnetic Properties.** The magnetic properties of **1**, in the form of  $\chi_M T$  versus  $T$ , are represented for the value

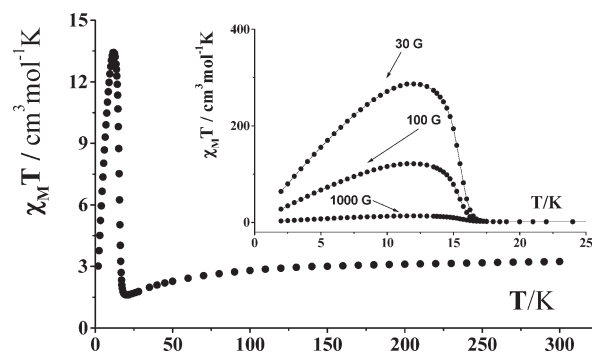


**Figure 5.** Plot of  $\chi_M T$  vs  $T$  in the 300–2 K range of temperatures for  $[\text{Co}_2(\text{N}_3)_4(\text{HMTA})(\text{H}_2\text{O})]_n$  (**1**) measured under an external magnetic field of 1000 G. Inset: Plot of  $\chi_M T$  vs  $T$  in the 25–2 K range of temperatures for **1** measured under external magnetic fields of 30, 100, and 1000 G.

of the applied magnetic field of 1000 G (Figure 5). The room temperature  $\chi_M T$  value of  $3.24 \text{ cm}^3 \text{ mol}^{-1} \text{ K}$  is smaller than the spin only value of  $3.750 \text{ cm}^3 \text{ mol}^{-1} \text{ K}$  for two uncoupled  $S = 3/2$  Co(II) ions. Upon lowering the temperature,  $\chi_M T$  decreases slowly, attains a minimum at 20 K ( $\chi_M T = 1.61 \text{ cm}^3 \text{ mol}^{-1} \text{ K}$ ) and shows an abrupt increase to a maximum value of  $13.43 \text{ cm}^3 \text{ mol}^{-1} \text{ K}$  at 12 K before decreasing in the lowest temperature region. At the same temperature, the  $\chi_M T$  value is  $287 \text{ cm}^3 \text{ mol}^{-1} \text{ K}$  at the applied field of 30 G. The magnetic susceptibility in the 25–300 K range obeys the Curie–Weiss law. The Curie–Weiss fitting of  $\chi_M^{-1}$  data above 25 K provides  $C = 3.53 \text{ cm}^3 \text{ mol}^{-1} \text{ K}$  and  $\theta = -26.62 \text{ K}$ , Figure 6. The continuous decrease in  $\chi_M T$  from room temperature to 20 K can be attributed to both the spin–orbit coupling of the octahedral Co(II) ions with a  $^4\text{T}_{1g}$  ground term and the moderate antiferromagnetic coupling between the Co(II) centers through the  $\mu_{1,3}$ -azido bridging ligands. Below 20 K, where an abrupt increase in  $\chi_M T$  versus  $T$  is observed, the susceptibility becomes field dependent, thus suggesting a ferromagnetic phase transition. Both the in-phase ( $\chi_M'$ ) and out-of-phase ( $\chi_M''$ ) alternating current (ac) susceptibility signals, Figure 7, which are frequency independent, show a sharp peak at  $T_c = 15.6 \text{ K}$  ( $T_c =$  Curie temperature), confirming the presence of net magnetization. At 2 K, **1** exhibits a magnetic hysteresis loop (Figure 8) with a large coercive field of 4700 G and a remnant magnetization of  $0.27 \text{ N}\beta$ . The magnetization at 2 K increases slowly with the increasing of the magnetic field, Figure 9, attaining a highest value at 5 T of  $0.70 \text{ N}\beta$ , which is significantly below the theoretical saturation magnetization of  $3 \text{ N}\beta$  for an isotropic high spin Co(II). Zero-field-cooled and field cooled magnetization (ZFCM/FCM) of **1** have been measured at 10 Oe

(36) O’Keeffe, M.; Peskov, M. A.; Ramsden, S.; Yaghi, O. M. *Acc. Chem. Res.* **2009**, *41*, 1782.

(37) Carlucci, L.; Ciani, G.; Proserpio, D. M.; Sironi, A. *Inorg. Chem.* **1997**, *36*, 1736.

(38) Blatov, V. A.; Carlucci, L.; Ciani, G.; Proserpio, D. M. *CrystEngComm* **2004**, *6*, 377–395.

(39) Baburin, I. A.; Blatov, V. A.; Carlucci, L.; Ciani, G.; Proserpio, D. M. *Cryst. Growth Des.* **2008**, *8*, 519–539.

(40) Baburin, I. A.; Blatov, V. A. *Acta Crystallogr., Sect. B: Struct. Sci.* **2007**, *63*, 791–802.

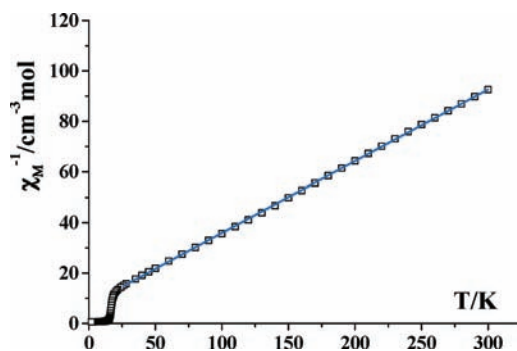


**Figure 6.** Plot of  $\chi_M^{-1}$  vs  $T$  in the 300–2 K range of temperatures for  $[\text{Co}_2(\text{N}_3)_4(\text{HMTA})(\text{H}_2\text{O})]_n$  (**1**) measured under external magnetic field of 1000 G. The solid line shows the best fit in the high-temperature region as Curie–Weiss law (see text).

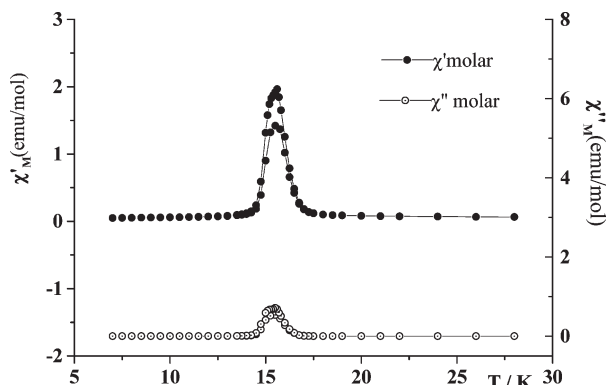


**Figure 7.** Temperature dependence of real and imaginary components of the ac susceptibility in zero applied static field with an oscillating field of 4 Oe at a frequencies of 122 and 997 Hz. The lines are guides.

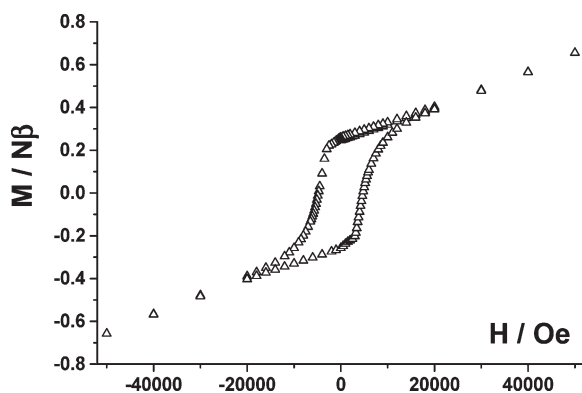


**Figure 8.**  $M-H$  curve of **1** measured at 2 K.

and are plotted in Figure 10. The ZFCM curve increases as the temperature rises from 2 K, reaches the maximum at 15.2 K, and then decreases quickly, which reveals the antiferromagnetic intrinsic state. As the sample cools, the FCM curve increases rapidly and diverges with the ZFCM curve around 16 K, which indicates the existence of spontaneous ferromagnetic ordering.

The reported magnetic properties (negative Weiss constant, hysteresis loop at 2K, abrupt increase in  $\chi_M T$  versus  $T$  below 20 K and no saturation limit) are

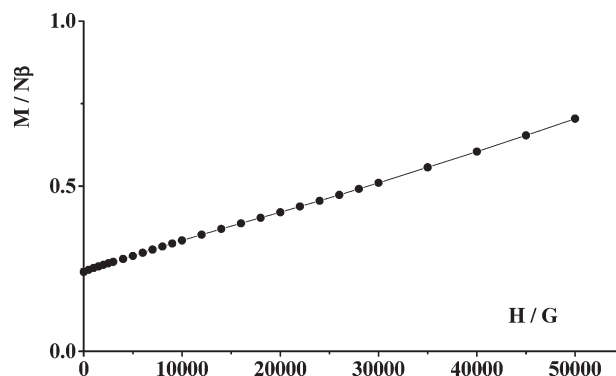


**Figure 9.** Field dependent magnetization at 2 K for **1**.

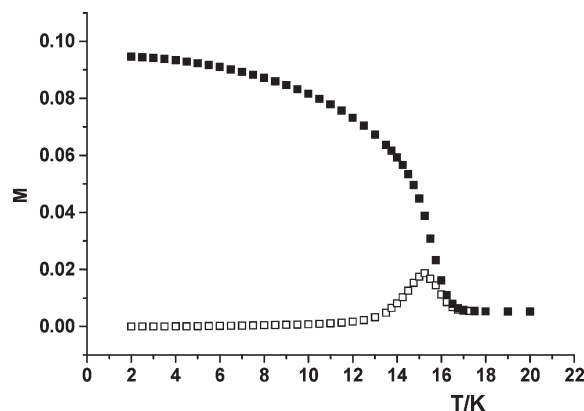


**Figure 10.** FC and ZFC magnetization vs  $T$  plots of compound **1** in an applied field of 10 Oe.

characteristic of spin canted antiferromagnetism, leading to weak ferromagnetism.<sup>41,42</sup> In the description of the structure, the magnetic network is a 3D structure of parallel sheets built from decanuclear Co(II) rings (see Figure 3, right). In a plane, the spin distribution is shown in Figure 11 and, in the ground state in the idealized structure,  $S$  for the sheet should be zero. It should be stressed that the azido bridged sheet described in Figure 11 is also a new 2D topology in the polynuclear azido-bridged Co(II) and Mn(II) compounds.<sup>1–17,43</sup> The planes in **1** are AF coupled by EE azido bridges and, for the idealized structure,  $S$  in the ground state for the 3D compound should be also zero.

The observed high values of the magnetization below the critical temperature may be attributed to the single ion magnetic anisotropy of the octahedral Co(II) ions and to the alternation of the relative orientation of adjacent metal chromophores in the planes:<sup>42</sup> the local spins in the ordered magnetic state are not parallel, but are canted (spin canting).<sup>44</sup> In the structure of **1**, the **Co1/Co1A** (basal azide plane of the dimeric di-EO-azide bridged Co octahedra) forms an interplanar angle of  $18.6^\circ$  with the  $a/b$  plane. The interplanar angle of **Co1/Co1A** (basal azide plane of the dimeric di-EO-azide bridged Co octahedra) with the basal Co-azide plane of **Co2** octahedron is  $120.9^\circ$ , Figure 1a. The angle of basal

(42) Rodríguez, A.; Kivekäs, R.; Colacio, E. *Chem. Commun.* **2005**, 5228.

(43) Ribas, J.; Escuer, A.; Monfort, M.; Vicente, R.; Cortés, R.; Lezama, L.; Rojo, T. *Coord. Chem. Rev.* **1999**, 193–195, 1027.

(44) Kahn, O. *Molecular Magnetism*; VCH Publishers, Inc: New York, 1993; pp 321–325.

(41) Retting, S. J.; Thompson, R. C.; Trotter, J.; Xia, S. *Inorg. Chem.* **1999**, 38, 1360.

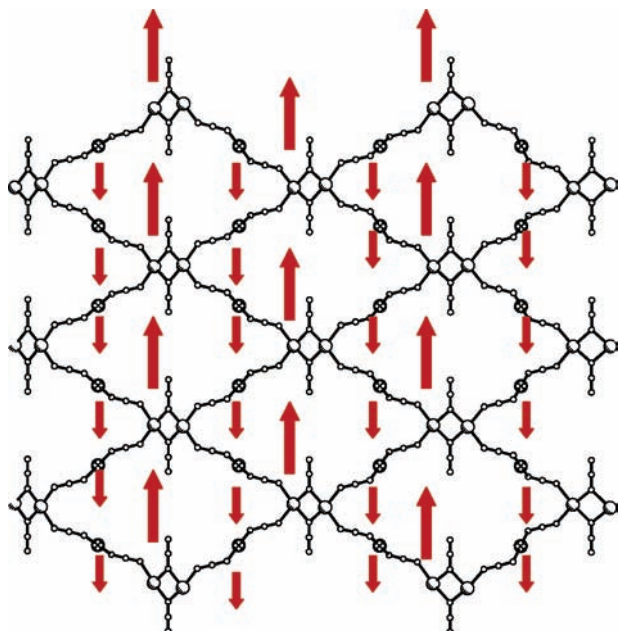


**Figure 11.** Co(II)-azido sublattice of **1**: View onto sheets of decanuclear rings oriented along [010] and [102] directions (compare with Figure 1c and Figure 3). Spin pattern within sheets of decanuclear rings. Along [100] (i.e.: *a*-axis of the unit cell) the Co2 centers of these sheets are antiferromagnetically coupled by single EE azide bridges to form the 3D network. As a consequence adjacent sheets have opposite spin orientations. (See also Figure 1c).

plane of **Co2** octahedron with that of the **Co2C** or **Co2E** octahedron is  $76.9^\circ$ . The torsion angles are  $\text{Co1-N21}\cdots\text{N23-Co2} = 83.9^\circ$ ;  $\text{Co2-N31}\cdots\text{N31E-Co2E} = 118.4^\circ$ , and  $\text{N2F-Co2}\cdots\text{Co2E-N2K} = 110.0^\circ$ . The canting angle  $\gamma$  at 2 K can be roughly estimated as  $7.2^\circ$  from the remnant magnetization of the powder sample,

$M_R^P$ , through the equation  $\sin(\gamma) = M_R^P/gSN\beta$ .<sup>11</sup> For octahedral  $\text{Co}^{2+}$  at 2 K, the effective spin of 1/2 is used with a common value of  $g = 4.3$ . Taking into account the complex 3D structure of **1**, the canting angle of  $7.2^\circ$  serves only for comparative purposes.

### Conclusion

In this paper we have described the synthesis and structural characterization of a new azido bridged 3D compound derived from the anisotropic Co(II) cation by using also the polydentate HMTA ligand. The formula of the compound is  $[\text{Co}_2(\text{N}_3)_4(\text{HMTA})(\text{H}_2\text{O})]_n$  (**1**) and shows a complex 3D structure in which Co(II) atoms linked by end-to-end azido bridging ligands coexist with end-on azido bridging ligands and with the HMTA ligand acting as tridentate bridging ligand. The coordination network formed in **1** is of a new three- and six connected topology (**loh1**), and the magnetic three- and four-connected 3D-net is of the highly symmetric **tfo** topology, not previously reported, that could serve as a blue print for other coordination polymers and MOFs through readily available square planar and trigonal SBUs. From the magnetic point of view, in the high temperature region **1** obeys the Curie–Weiss law but shows magnetic ordering at low temperature because of the Co(II) anisotropy and the canting effect.

**Acknowledgment.** This research was partially supported by CICYT (Grant CTQ2006-01759) and the Swedish Research Council (VR Grant 2007-4412). F.A.M. thanks Dr. J. Baumgartner (TU Graz), for assistance.

**Supporting Information Available:** Tables of X-ray crystallographic data in CIF format for the structure reported in this paper. This material is available free of charge via the Internet at <http://pubs.acs.org>.